

Electronic viscosity and energy relaxation in neutral graphene

Vanessa Gall,^{1,2} Boris N. Narozhny,^{2,3} and Igor V. Gornyi^{1,2,4}

¹*Institute for Quantum Materials and Technologies, Karlsruhe Institute of Technology, 76021 Karlsruhe, Germany*

²*Institut für Theorie der Kondensierten Materie, Karlsruhe Institute of Technology, 76128 Karlsruhe, Germany*

³*National Research Nuclear University MEPhI (Moscow Engineering Physics Institute), 115409 Moscow, Russia*

⁴*Ioffe Institute, 194021 St. Petersburg, Russia*

(Dated: August 30, 2022)

We explore hydrodynamics of Dirac fermions in neutral graphene in the Corbino geometry. In the absence of magnetic field, the bulk Ohmic charge flow and the hydrodynamic energy flow are decoupled. However, the energy flow does affect the overall resistance of the system through viscous dissipation and energy relaxation that has to be compensated by the work done by the current source. Solving the hydrodynamic equations, we find that local temperature and electric potential are discontinuous at the interfaces with the leads as well as the device resistance and argue that this makes Corbino geometry a feasible choice for an experimental observation of the Dirac fluid.

Quantum dynamics of charge carriers is one of the most important research directions in condensed matter physics. In many materials transport properties can be successfully described under the assumption of weak electron-electron interaction allowing for free-electron theories [1]. An extension of this approach to strongly-correlated systems remains a major unsolved problem. The advent of “ultra-clean” materials poses new challenges, especially if the electronic system is nondegenerate. At high temperatures such systems may exhibit signatures of a collective motion of charge carriers resembling the hydrodynamic flow of a viscous fluid [2–14].

Electronic viscosity has been discussed theoretically for a long time [15–20], but became the subject of dedicated experiments [2, 9] only recently, after ultra-clean materials became available. Up until now, most experimental efforts were focusing on graphene [2–11] where the hydrodynamic regime is apparently easier to achieve [21, 22]. Viscous effects manifest themselves in nonuniform flows. In the common “linear” geometry (channels, wires, Hall bars, etc.) this occurs in “narrow” samples where the typical length scale associated with viscosity is of the same order as the channel width [23–27]. In contrast, in the “circular” Corbino geometry, see Fig. 1, the electric current is nonuniform even in the simplest Drude picture (in the absence of magnetic field, $\mathbf{j} \propto \mathbf{e}_r/|\mathbf{r}|$, where $\mathbf{e}_r = \mathbf{r}/|\mathbf{r}|$) making it an excellent platform to measure electronic viscosity [28–31]. In the last year, electronic hydrodynamics in the Corbino geometry has been studied both experimentally [32] and theoretically [33–36].

In this paper we address the “Dirac fluid” [3, 9] (the hydrodynamic flow of charge carriers in neutral graphene) in the Corbino geometry. Unlike doped graphene where degenerate, Fermi-liquid-like electrons may be described by the Navier-Stokes equation with a weak damping term due to disorder [16, 21, 23], the two-band physics of neutral graphene leads to unconventional hydrodynamics [22, 37]. In the hydrodynamic approach any macroscopic current can be expressed as a product of the corresponding density and hydrodynamic velocity \mathbf{u} (up to dissi-

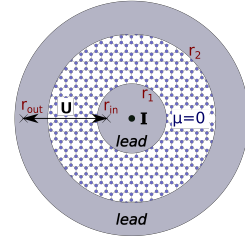


FIG. 1. Corbino geometry: the annulus-shaped sample of neutral graphene ($\mu = 0$) is placed between the two leads: the inner circle of the radius r_1 and the outer shell with the inner radius r_2 . A current I is injected through at the center point and a voltage U is measured between electrodes placed at the inner and outer radius r_{in} and r_{out} .

pative corrections), e.g., the electric and energy current densities are $\mathbf{j} = n\mathbf{u}$ and $\mathbf{j}_E = n_E\mathbf{u}$, respectively. In the degenerate regime the charge and energy densities are proportional to each other (to the leading approximation in thermal equilibrium $n_E = 2\mu n/3$, where μ is the chemical potential) and the two currents are equivalent [38]. In contrast, the equilibrium charge density vanishes at charge neutrality, $n(\mu = 0) = 0$, while the energy density remains finite. The two currents “decouple”: the energy current remains “hydrodynamic”, the charge current is completely determined by the dissipative correction $\delta\mathbf{j}$.

Electronic transport at charge neutrality has been a subject of intensive research [9, 24–27, 38–46] leading to general consensus on the basic result: in the absence of magnetic field, $\mathbf{B} = 0$, resistivity of neutral graphene is determined by the electron-electron interaction

$$R_0 = \frac{\pi}{2e^2 T \ln 2} \left(\frac{1}{\tau_{11}} + \frac{1}{\tau_{\text{dis}}} \right) \xrightarrow{\tau_{\text{dis}} \rightarrow \infty} \frac{1}{\sigma_Q}. \quad (1)$$

Here $\tau_{11} \propto \alpha_g^{-2} T^{-1}$ describes the appropriate electron-electron collision integral and σ_Q is the “intrinsic” or “quantum” conductivity of graphene. Disorder scattering is characterized by the mean free time τ_{dis} , which is large under the assumptions of the hydrodynamic regime,

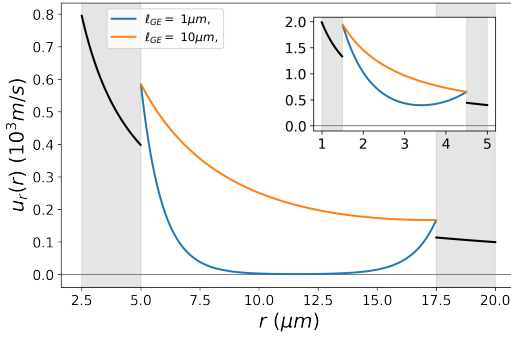


FIG. 2. Radial component of the hydrodynamic velocity u_r . Black lines show the drift velocity in the leads, $u_r^{\text{in(out)}} \propto 1/r$. Colored curves correspond to the solution Eq. (4) for the two indicated values of ℓ_{GE} . The results are plotted for the two cases of a large (main panel) and small (inset) device.

$\tau_{\text{dis}} \gg \tau_{11}$ and yields a negligible contribution to Eq. (1). Equation (1) describes the uniform bulk current and is independent of viscosity (i.e., in a channel [21, 24, 44, 46]). In contrast, in the Corbino geometry the current flow is necessarily inhomogeneous and hence viscous dissipation must be taken into account.

We envision the following experiment: a graphene sample (at charge neutrality) in the shape of an annulus is placed between the inner (a disk of radius r_1) and outer (a ring with the inner radius r_2) metallic contacts (leads). For simplicity, we assume both leads to be of the same material, e.g., highly doped graphene with the same doping level. The electric current I is injected into the center of the inner lead preserving the rotational invariance (e.g., through a thin vertical wire attached to the center point) and spreads towards the outer lead, which for concreteness we assume to be grounded. The overall voltage drop U is measured between two points in the two leads (at the radii $r_{\text{in}} < r_1$ and $r_{\text{out}} > r_2$) yielding the device resistance, $R = U/I$. In most traditional measurements, the leads' resistance is minimal, while the contact resistance is important only in ballistic systems, see e.g., Ref. [10]. Hence, one may interpret the measured voltage drop in terms of resistivity of the sample material. Here we focus on the device resistance and show that in the hydrodynamic regime there is an additional contribution due to electronic viscosity and energy relaxation.

Charge flow through the Corbino disk can be described as follows. The injected current spreads through the inner lead according to the Ohm's law and continuity equation. In the stationary case, the latter determines the radial component of the current density, $j_r^{\text{in}} = I/(2\pi er)$. This defines the drift velocity $\mathbf{u}^{\text{in}} = \mathbf{j}^{\text{in}}/n^{\text{in}}$ (n^{in} is the carrier density in the inner lead) and the energy current $\mathbf{j}_E^{\text{in}} = n_E^{\text{in}} \mathbf{u}^{\text{in}}$. Reaching the interface, both currents continue to flow into the graphene sample. Here (at $n = 0$ and $\mathbf{B} = 0$) the energy current $\mathbf{j}_E = n_E \mathbf{u}$ is decoupled from the electric current $\mathbf{j} = \delta \mathbf{j}$. Charge conservation

requires the radial component of the electric current to be continuous at the interface, $\delta \mathbf{j}(r_1) = \mathbf{j}^{\text{in}}(r_1)$. Due to the continuity equation, the current density in graphene has the same functional form, $\delta j_r = I/(2\pi er)$. Does this mean that the device resistance trivially follows if one knows the resistivity of graphene? The answer is “no”, since the electrochemical potential is discontinuous at the interface! There are two mechanisms for the “jump” of the potential: (i) the usual Schottky contact resistance [42, 47], and (ii) dissipation due to viscosity [31] and energy relaxation [48]. Since the lost energy must come from the current source, both contribute to R .

The energy flow in neutral graphene is described by the set of hydrodynamic equations developed in Refs. [37, 44, 48] and most recently solved in Ref. [46] in the channel geometry. Within linear response, the equations are

$$\nabla \cdot \delta \mathbf{j} = 0, \quad (2a)$$

$$n_I \nabla \cdot \mathbf{u} + \nabla \cdot \delta \mathbf{j}_I = -(12 \ln 2 / \pi^2) n_I \mu_I / (T \tau_R), \quad (2b)$$

$$\nabla \delta P = \eta \Delta \mathbf{u} - 3P \mathbf{u} / (v_g^2 \tau_{\text{dis}}), \quad (2c)$$

$$3P \nabla \cdot \mathbf{u} = -2\delta P / \tau_{RE}. \quad (2d)$$

Here Eq. (2a) is the continuity equation; Eq. (2b) is the “imbalance” continuity equation [37, 42] (μ_I is the imbalance chemical potential, $n_I = \pi T^2 / (3v_g^2)$ is the equilibrium imbalance density, v_g is the band velocity in graphene, and τ_R is the recombination time); Eq. (2c) is the linearized Navier-Stokes equation [37, 46, 49, 50]; and Eq. (2d) is the linearized “thermal transport” equation (τ_{RE} is the energy relaxation time [48]). Equilibrium thermodynamic quantities (the pressure $P = 3\zeta(3)T^3 / (\pi v_g^2)$, enthalpy density \mathcal{W} , and energy density are related by the “equation of state”, $\mathcal{W} = 3P = 3n_E/2$). The dissipative corrections to the macroscopic currents are given by

$$\delta \mathbf{j} = \mathbf{E} / (eR_0), \quad (3a)$$

$$\delta \mathbf{j}_I = -\frac{2\gamma \ln 2}{\pi} T \tau_{\text{dis}} \nabla \mu_I, \quad \gamma = \frac{\delta_I}{1 + \tau_{\text{dis}} / (\delta_I \tau_{22})}, \quad (3b)$$

where $\tau_{22} \propto \alpha_g^{-2} T^{-1}$ describes a component of the collision integral that is qualitatively similar, but quantitatively distinct from τ_{11} and $\delta_I \approx 0.28$. The equations (2) and (3) should be solved for \mathbf{u} , $\delta \mathbf{j}$, $\delta \mathbf{j}_I$, \mathbf{E} , μ_I , and δP .

Excluding δP from Eqs. (2c) and (2d) we find a second-order differential equation for \mathbf{u}

$$\eta' \Delta \mathbf{u} = 3P \mathbf{u} / (v_g^2 \tau_{\text{dis}}), \quad \eta' = \eta + 3P \tau_{RE} / 2. \quad (4a)$$

In the Corbino disk, the general solution for the radial component of the velocity has the form

$$u_r = a_1 I_1 \left(\frac{r}{\ell_{GE}} \right) + a_2 K_1 \left(\frac{r}{\ell_{GE}} \right), \quad \ell_{GE}^2 = \frac{v_g^2 \eta' \tau_{\text{dis}}}{3P}, \quad (4b)$$

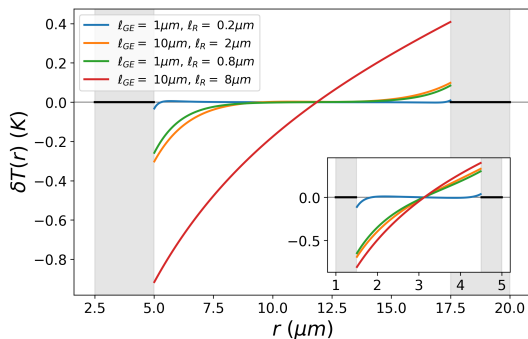


FIG. 3. Temperature distribution in the device. Colored curves correspond to the solution of the hydrodynamic equations for the indicated values of ℓ_{GE} and ℓ_R . The results are plotted for the two cases of a large (main panel) and small (inset) device. In the leads $\delta T = 0$, shown by black lines.

where $I_1(z)$ and $K_1(z)$ are the Bessel functions. The coefficients a_1 and a_2 can be found using the continuity of the entropy current at the two interfaces (within linear response). The resulting behavior is shown in Fig. 2 (here we choose to show our results in graphical form since the analytic expressions are somewhat cumbersome [51]; quantitative calculations were performed for $T = 100$ K and experimentally relevant values of the parameters taken from Refs. [8–10, 48]).

In the hydrodynamic regime, the electron-electron scattering time is the shortest scale in the problem, hence the spatial variation of \mathbf{u} is determined by energy relaxation. If $\ell_{GE} \ll r_{\text{out}} - r_{\text{in}}$, then the energy current injected from the leads decays in a (relatively small) boundary region while in the bulk of the sample $\mathbf{u} \rightarrow 0$. On the other hand, if ℓ_{GE} is of the same order as (or larger than) the system size, then u_r does not vanish and approaches the standard Corbino profile, $u_r \propto 1/r$. At each interface, u_r exhibits a jump due to the mismatch of the entropy densities in the sample and leads.

The nonequilibrium quantities δP and μ_I can now be found straightforwardly. The former follows directly from Eq. (2d) using the solution (4), while the differential equation for the latter can be found by substituting Eq. (3b) into Eq. (2b) and using the solution (4). The boundary conditions for δP and μ_I follow from the continuity equations for the charge and imbalance. The two quantities can be combined to determine the nonequilibrium temperature variation, δT , shown in Fig. 3. For a large sample ($\ell_{GE}, \ell_R \ll r_{\text{out}} - r_{\text{in}}$, $\ell_R^2 = \gamma v_g^2 \tau_{\text{dis}} \tau_R / 2$), δT exhibits fast decay and vanishes in the bulk of the sample. For larger values of ℓ_{GE}, ℓ_R energy relaxation is less effective and the system exhibits an inhomogeneous temperature profile.

The obtained solutions completely describe the hydrodynamic energy flow in neutral graphene. Our remaining task is to find the behavior of the electrochemical potential at the two interfaces enabling us to determine R .

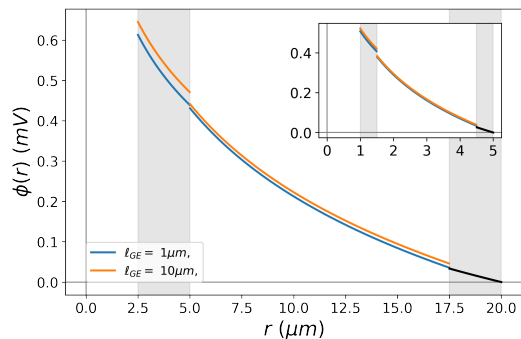


FIG. 4. Electrochemical potential (voltage drop) throughout the device. The black line shows the Ohmic behavior in the outer lead relative to the ground. The jumps at the interfaces are due to dissipative effects (viscosity and energy relaxation) in the bulk of the sample.

The standard description of interfaces between metals or semiconductors [47] can be carried over to neutral graphene [42] in terms of the contact resistance. Typically, this is a manifestation of the difference of work functions of the two materials across the interface. In graphene, the contact resistance was recently measured in Ref. [10], see also Refs. [32, 52, 53]. In the standard diffusive (or Ohmic) case, the contact resistance leads to a voltage drop that is small compared to the voltage drop in the bulk of the sample and can be ignored. In contrast, in the ballistic case there is almost no voltage drop in the bulk, such that most energy is dissipated at the contacts. Both scenarios neglect electron-electron interactions.

In the diffusive case interactions lead to corrections to the bulk resistivity [54, 55] and the contact resistance can still be ignored. In the ballistic case electron-electron interaction may give rise to a “Knudsen-Poiseuille” crossover [16] and drive the electronic system to the hydrodynamic regime. While the Ohmic resistivity of the electronic fluid may remain small, the hydrodynamic flow possesses another channel for dissipation through viscosity [31]. At charge neutrality, this effect is subtle, since the electric current is decoupled from the hydrodynamic energy flow, see Eq. (3a). At the same time, both are induced by the current source providing the energy dissipated not only by Ohmic effects, but also by viscosity [31] and energy relaxation processes [48] that should be taken into account in the form of an additional voltage drop. Since the voltage drop in the bulk of the sample is completely determined by Eq. (3a), the additional contribution takes the form of a jump in ϕ at the interface corresponding to an excess electric field induced in the thin Knudsen layer around the interface [31].

The magnitude of the jump in ϕ can be established by considering the flow of energy through the interface. Following the standard route [31, 56], we consider the time derivative of the kinetic energy, $\mathcal{A} = \dot{\mathcal{E}}$, where \mathcal{E} is obtained by integrating the energy density $n_E(\mathbf{u}) - n_E(0)$

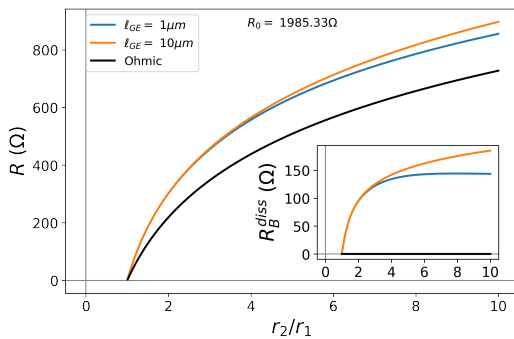


FIG. 5. Total resistance of the Corbino device for different values of ℓ_{GE} (here $r_1 = 0.5 \mu\text{m}$). Inset: additional contribution to the resistance due to viscous dissipation.

over the volume. Working within linear response, we expand the latter to the leading order in the hydrodynamic velocity. Finding time derivatives from the equations of motion and using the continuity equation and partial integration, we then separate the “bulk” and “boundary” contributions, $\mathcal{A} = \mathcal{A}_{\text{bulk}} + \mathcal{A}_{\text{edge}}$. We interpret the former as the bulk dissipation, while $\mathcal{A}_{\text{edge}}$ includes the energy brought in (carried away) through the boundary by the incoming (outgoing) flow. In the stationary state $\dot{\mathcal{E}} = 0$, dissipation is balanced by the work done by the source. Assuming that no energy is accumulated at the interface, we find the corresponding boundary condition.

The specific form of the equations of motion depends on the choice of the material. Assuming the leads’ material is highly doped graphene, the equation of motion is the usual Ohm’s law with the diffusion term [57] coming from the gradient of the stress-energy tensor [38], here we include a viscous contribution due to disorder [58] and find [31] (omitting the continuous entropy flux)

$$\mathcal{A}_{\text{edge}}^{\text{lead}} = \int dS_{\beta} \left(u_{\alpha}^L \sigma'_{L;\alpha\beta} - u_{\beta}^L \delta P_L - e j_{\beta}^L \phi \right), \quad (5a)$$

where $\mathbf{j}^L = n_L \mathbf{u}^L$ is the current density, \mathbf{u}^L is the drift velocity, δP_L is the nonequilibrium pressure, and σ'_L is the viscous stress tensor in the lead. The first two terms are the usual dissipative contributions to the energy flow across the boundary [56], the last term is the Joule heat.

In neutral graphene, we obtain similar results from the Navier-Stokes equation, except that the Joule heat is now determined by $\delta \mathbf{j}$

$$\mathcal{A}_{\text{edge}}^{\text{sample}} = \int dS_{\beta} \left(u_{\alpha} \sigma'_{\alpha\beta} - u_{\beta} \delta P - e \delta j_{\beta} \phi \right). \quad (5b)$$

Equating the two contributions (5) and using the above solutions for the velocity and pressure, we find the jumps of the potential ϕ at the two interfaces. This allows us to determine ϕ everywhere in the device, see Fig. 4, as well as the device resistance.

The total resistance of the Corbino device is shown in Fig. 5. Neglecting hydrodynamic effects, we find the

usual logarithmic dependence of R on the system size. Viscosity and energy relaxation provide an additional dissipation channel and hence increase R . Energy relaxation contributes to this increase since it dominates the hydrodynamic energy flow, see Eq. (4). At the same time, the boundary condition for the electric potential, Eqs. (5), is determined by viscosity.

In this paper we have solved the hydrodynamic equations in neutral graphene. We have shown, that despite the known decoupling of the Ohmic charge flow and hydrodynamic energy flow, in Corbino geometry the latter does affect the observable behavior leading to jumps in temperature (shown in Fig. 3) and the electric potential, see Fig. 4. The potential jump is distinct from the usual contact resistance insofar it is a function of the system size. Both effects are observable using the modern imaging techniques (the local temperature variation can be measured using the approach of Refs. [59–61], while measurements of the local potential are at the heart of the technique proposed in Refs. [10, 62]). Hydrodynamics also affects the more conventional transport measurements through the size-dependent contribution to the device resistance, see Fig. 5.

Our results highlight several particular features of the Dirac fluid in neutral graphene. Firstly, the “linear response” currents (3) are independent of the temperature gradient due to exact particle-hole symmetry [42]. Secondly, in contrast to the case of doped graphene [31] *the Dirac fluid is compressible* even within linear response (due to energy relaxation, see Eq. (2d)). Finally, the hydrodynamic flow in neutral graphene is the energy flow. Hence, energy relaxation effectively dominates over viscous effects, see Eqs. (4), complicating experimental determination of η .

External magnetic field is also known to couple the charge and energy flows in neutral graphene [37]. We expect that our theory will yield interesting results on Corbino magnetoresistance [52]. Another extension of our theory is the study of thermoelectric phenomena, which is more interesting if one moves away from the neutrality point [34] (where the thermopower must vanish due to the exact particle-hole symmetry). Our results on both issues will be reported elsewhere.

The authors are grateful to P. Hakonen, V. Kachorovskii, A. Levchenko, A. Mirlin, J. Schmalian, A. Shnirman, and M. Titov for fruitful discussions. This work was supported by the German Research Foundation DFG within FLAG-ERA Joint Transnational Call (Project GRANSFORT), by the European Commission under the EU Horizon 2020 MSCA-RISE-2019 Program (Project 873028 HYDROTRONICS), by the German Research Foundation DFG project NA 1114/5-1 (BNN), and by the German-Israeli Foundation for Scientific Research and Development (GIF) Grant No. I-1505-303.10/2019 (IVG).

Supplemental material

Starting with the general form of the hydrodynamic equations in graphene, we obtain the analytical results presented graphically in the main text. In Sec. we summarize the hydrodynamic equations for graphene. In Sec. we specify these equations within linear response in polar coordinates at charge neutrality and $B = 0$. In Sec. we formulate a description of the leads followed by the relevant boundary conditions at the lead-graphene interfaces in Sec. . Next, in Sec. we present the full analytical solution for the hydrodynamic equations in the Corbino geometry with the above boundary conditions. In Sec. we discuss the dissipation in the system and corroborate the argument used in the main text to obtain the device resistance. Finally, we conclude with a brief analysis in Sec. .

Electronic hydrodynamics in graphene

Following Ref. [63] we combine the chemical potentials of the two bands in graphene μ_{\pm} into

$$\mu = (\mu_+ + \mu_-)/2, \quad \mu_I = (\mu_+ - \mu_-)/2 \quad (6)$$

and introduce their conjugate charge and imbalance densities

$$n = n_+ - n_-, \quad n_I = n_+ + n_-. \quad (7)$$

Taking into account dissipative corrections due to electron-electron collisions we then obtain the electric (\vec{j}) and imbalance (\vec{j}_I) currents as

$$\vec{j} = n\vec{u} + \delta\vec{j}, \quad \vec{j}_I = n_I\vec{u} + \delta\vec{j}_I, \quad (8)$$

where \vec{u} is the drift velocity. The energy current $\vec{j}_E = n_E\vec{u}$ is proportional to the momentum density and is not relaxed by electron-electron collisions. The currents \vec{j} and \vec{j}_I satisfy the continuity equations

$$\partial_t n + \vec{\nabla} \cdot \vec{j} = 0, \quad (9a)$$

which describes the exact conservation of charge and

$$\partial_t n_I + \vec{\nabla} \cdot \vec{j}_I = -\frac{n_I - n_{I,0}}{\tau_R} = -\frac{12 \ln 2}{\pi^2} \frac{n_{I,0} \mu_I}{T \tau_R}, \quad (9b)$$

where $n_{I,0} = \pi T^2 / (3v_g^2)$ is the equilibrium value of the total quasiparticle density (at $\mu_I = 0$) and τ_R is the recombination time.

A similar equation can be formulated for the energy density

$$\partial_t n_E + \vec{\nabla} \cdot \vec{j}_E = e\vec{j} \cdot \vec{E} - \frac{n_E - n_{E,0}}{\tau_{RE}}, \quad (9c)$$

where τ_{RE} is the energy relaxation time. Typically this is replaced by the thermal transport equation

$$\begin{aligned} T \left[\frac{\partial s}{\partial t} + \vec{\nabla}_{\vec{r}} \cdot \left(s\vec{u} - \delta\vec{j} \frac{\mu}{T} - \delta\vec{j}_I \frac{\mu_I}{T} \right) \right] &= \delta\vec{j} \cdot \left[e\vec{E} + \frac{e}{c} \vec{u} \times \vec{B} - T \vec{\nabla} \frac{\mu}{T} \right] - T \delta\vec{j}_I \cdot \vec{\nabla} \frac{\mu_I}{T} \\ &+ \frac{\eta}{2} \left(\nabla_{\alpha} u_{\beta} + \nabla_{\beta} u_{\alpha} - \delta_{\alpha\beta} \vec{\nabla} \cdot \vec{u} \right)^2 - \frac{n_E - n_{E,0}}{\tau_{RE}} + \mu_I \frac{n_I - n_{I,0}}{\tau_R} + \frac{\mathcal{W} \vec{u}^2}{v_g^2 \tau_{\text{dis}}}. \end{aligned} \quad (9d)$$

Within linear response the two equations coincide. Finally, the generalized Navier-Stokes equation is given by

$$\mathcal{W}(\partial_t + \vec{u} \cdot \vec{\nabla})\vec{u} + v_g^2 \vec{\nabla} P + \vec{u} \partial_t P + e(\vec{E} \cdot \vec{j})\vec{u} = v_g^2 \left[\eta \Delta \vec{u} - \eta_H \Delta \vec{u} \times \vec{e}_B + en\vec{E} + \frac{e}{c} \vec{j} \times \vec{B} \right] - \frac{\vec{j}_E}{\tau_{\text{dis}}}. \quad (9e)$$

Here η and η_H are the shear and Hall viscosity coefficients, respectively.

The expressions for the dissipative corrections can be found in the Appendix of Ref. [63].

Charge neutral Corbino disk at $B = 0$

Taking into account the rotational symmetry of the Corbino disk, we express the hydrodynamic theory in polar coordinates (r, ϑ) . All quantities can only depend on the radial component r . Within linear response and at $B = 0$, the hydrodynamic equations (9) can be transformed to

$$\frac{1}{r} \frac{\partial(r\delta j_r)}{\partial r} = 0, \quad (10a)$$

$$n_{I,0} \frac{1}{r} \frac{\partial(r u_r)}{\partial r} + \frac{1}{r} \frac{\partial(r\delta j_{Ir})}{\partial r} = -\frac{12 \ln 2}{\pi^2} \frac{n_{I,0} \mu_I(r)}{T \tau_R}, \quad (10b)$$

$$u_\vartheta = 0, \quad (10c)$$

$$\frac{\partial \delta P}{\partial r} = \eta \partial_r \left(\frac{1}{r} \frac{\partial(r u_r)}{\partial r} \right) - \frac{3P u_r}{v_g^2 \tau_{\text{dis}}}, \quad (10d)$$

$$3P \frac{1}{r} \frac{\partial(r u_r)}{\partial r} = -\frac{2\delta P(r)}{\tau_{RE}}. \quad (10e)$$

The electric field \vec{E} does not appear in Eqs. (10) due to charge neutrality. It does however determine the dissipative correction $\delta \vec{j}$ which at charge neutrality is the whole current. In the absence of the magnetic field, all currents are radial. In polar coordinates, the dissipative corrections take the form

$$\delta j_r = \frac{E_r(r)}{e R_0}, \quad (11a)$$

$$\delta j_\vartheta = 0, \quad (11b)$$

$$\delta j_{Ir} = -\frac{\delta_I}{\tau_{\text{dis}}^{-1} + \delta_I^{-1} \tau_{22}^{-1}} \frac{2T \ln 2}{\pi} \frac{\partial \mu_I}{\partial r}, \quad (11c)$$

$$\delta j_{I\vartheta} = 0. \quad (11d)$$

Equations (10) and (11) have to be solved together taking into account the corresponding boundary conditions see below.

For the purposes of establishing the boundary conditions we also need to specify the stress tensor. At $B = 0$ (and within linear response, meaning neglecting terms that are higher than the leading order in velocity or its derivatives), the stress tensor is

$$\Pi_E^{\alpha\beta} = P \delta^{\alpha\beta} - \sigma^{\alpha\beta}. \quad (12)$$

Since the Hall viscosity vanishes at charge neutrality (as well as at $B = 0$), the viscous stress tensor in Cartesian coordinates is given by

$$\sigma^{\alpha\beta} = \eta \left(\nabla^\alpha u^\beta + \nabla^\beta u^\alpha - \delta^{\alpha\beta} \vec{\nabla} \cdot \vec{u} \right), \quad (13)$$

which in polar coordinates becomes

$$\sigma_{rr} = -\sigma_{\vartheta\vartheta} = \eta \left(\partial_r - \frac{1}{r} \right) u_r, \quad \sigma_{r\vartheta} = \sigma_{\vartheta r} = \eta \left(\partial_r - \frac{1}{r} \right) u_\vartheta. \quad (14)$$

Description of leads

The leads, which are attached at the inner and outer radius of the Corbino disk, are assumed to be a normal metal in the degenerate regime ($\mu_L \gg T$), where transport is dominated by disorder scattering characterized by the relaxation time τ_L . In this case we may restrict ourselves to a single band, such that there is a single macroscopic current satisfying the continuity equation

$$\partial_t n_L + \vec{\nabla} \cdot \vec{j} = 0. \quad (15)$$

Within linear response, one can obtain the macroscopic equation of motion (or generalized Ohm's law) integrating the kinetic equation [64]. This way one finds

$$m \partial_t \vec{j} + \vec{\nabla} \check{\Pi}_E - e n_L \vec{E} - \frac{e}{c} \vec{j} \times \vec{B} = -\frac{m}{\tau_L} \vec{j}, \quad (16)$$

where the stress tensor may be expressed in terms of thermodynamic pressure and disorder-induced viscosity

$$\Pi_E^{\alpha\beta} = P \delta^{\alpha\beta} - \sigma^{\alpha\beta}, \quad \eta_L = \frac{\mu^3 \tau_L}{4\pi v_g^2 \hbar^2}. \quad (17)$$

To be concrete, we assume that the leads' material is doped graphene. In that case we may introduce the "effective mass" $m = \mu_L / v_g^2$ and the drift velocity \vec{u}_L , such that $\vec{j} = n_L \vec{u}_L$. Expressing the carrier density in terms of pressure, we find

$$m \vec{j} = \frac{3P_L}{v_g^2} \vec{u}_L, \quad (18)$$

where to lowest order in temperature we find $P_L = \mu^3 / (3\pi v_g^2 \hbar^2)$. In the stationary state and at $B = 0$, the equations of motion become

$$\vec{\nabla} \vec{u}_L = 0, \quad (19)$$

$$\vec{\nabla} \check{\Pi}_E + e n_L \vec{\nabla} \phi = -\frac{3P_L}{v_g^2 \tau_L} \vec{u}_L. \quad (20)$$

Experimentally, the density n_L and the chemical potential μ are fixed by the gate voltage. Moreover, under the common assumption of fast equilibration in the leads, we may assume a uniform temperature T as well. The general variation of P_L is found to be

$$\delta P_L = \left(\frac{2\pi\mu T \delta T}{3v_g^2} + \frac{\pi T^2 \delta \mu}{3v_g^2} + \frac{\mu^2 \delta \mu}{\pi v_g^2} \right) \quad (21)$$

and thus vanishes under the condition we consider. Since the leads are highly doped, we find $n_L = n_+ = n_-$, such that the imbalance chemical potential μ_I vanishes.

Boundary conditions

The differential equations (10) and (11) should be supplemented by a suitable set of boundary conditions. The only boundaries present in the Corbino are boundaries between the sample and the leads. Since charge conservation is exact and also holds in the leads, we find

$$j_r(r_1 - \epsilon) = \delta j_r(r_1 + \epsilon), \quad \delta j_r(r_2 - \epsilon) = j_r(r_2 + \epsilon). \quad (22)$$

Fixing the total current I in a radially symmetric system completely determines the current density

$$I = e \int d\vec{A} \cdot \vec{j} = 2\pi e r j_r. \quad (23)$$

In contrast, the total quasiparticle number (imbalance) and entropy are not conserved due to recombination and energy relaxation processes. However, assuming that the corresponding relaxation rates are not singular at the

interface, the continuity equations (9b) and (9d) yield the following boundary conditions for the radial components of the current densities.

The resulting boundary conditions at the two interfaces can be summarized as follows

$$j_r(r_1 - \epsilon) = n_L u_r(r_1 - \epsilon) = \delta j_r(r_1 + \epsilon), \quad (24)$$

$$j_{I,r}(r_1 - \epsilon) = n_L u_{L,r}(r_1 - \epsilon) = n_{I,0} u_r(r_1 + \epsilon) + \delta j_{I,r}(r_1 + \epsilon) = \delta j_r(r_1 + \epsilon), \quad (25)$$

$$s_L u_{L,r}(r_1 - \epsilon) = s_B u_r(r_1 + \epsilon) \quad (26)$$

$$j_r(r_2 + \epsilon) = n_L u_{L,r}(r_2 + \epsilon) = \delta j_r(r_2 - \epsilon), \quad (27)$$

$$j_{I,r}(r_2 + \epsilon) = n_L u_{L,r}(r_2 + \epsilon) = n_{I,0} u_r(r_2 - \epsilon) + \delta j_{I,r}(r_2 - \epsilon) = \delta j_r(r_2 - \epsilon), \quad (28)$$

$$s_L u_{L,r}(r_2 + \epsilon) = s_B u_r(r_2 - \epsilon). \quad (29)$$

Full solution

Solving the equations of motion in the leads, we find

$$u_{L,r} = \frac{I}{2\pi e n_L r}, \quad u_{L,\vartheta} = 0, \quad (30)$$

$$\sigma_{rr} = \frac{-I\eta_L}{\pi e n_L r^2}, \quad \sigma_{r\vartheta} = 0, \quad (31)$$

$$E_r = \frac{2P_L}{e n_L v_g^2 \tau_L} \frac{I}{2\pi e n_L r}, \quad (32)$$

$$\phi(r) = -\frac{I}{2\pi} \frac{2P_L}{e^2 n_L^2 v_g^2 \tau_L} \log\left(\frac{r}{r_0}\right). \quad (33)$$

Here the drift velocity follows from the continuity equation and the relation to the current which in turn is given by Eq. (23). After that, the assumption $\delta P = 0$ leads to the simple $1/r$ behavior for the electrical field E_r as well. Consequently, the charge density (from the Poisson equation) is indeed constant. On the other hand, the constant r_0 in the potential is not fixed by the boundary conditions we have imposed so far. Finally, neither the electric field nor the current depend on the disorder dominated viscosity η_L . However, the viscous stress tensor itself is not zero, which will be used below later.

The above expressions can be re-written in terms of the temperature T and the chemical potential μ_L in the leads. Under our assumptions, the leads' material is graphene, where the entropy density is defined as

$$Ts = 3P - \mu n - \mu_I n_I. \quad (34)$$

For $\mu \gg T$ in the leads we then find

$$P_L = \frac{\pi T^2 \mu}{3v_g^2} + \frac{\mu^3}{3\pi v_g^2} = P_L^T + P_L^{T=0}, \quad (35)$$

$$n_L = \frac{\pi T^2}{3v_g^2} + \frac{\mu^2}{\pi v_g^2} \quad (36)$$

$$s_L T = 3P_L - n_L \mu = \frac{\pi T^2 \mu}{v_g^2} + \frac{\mu^3}{\pi v_g^2} - \frac{\pi T^2 \mu}{3v_g^2} - \frac{\mu^3}{\pi v_g^2} = \frac{2}{3} \frac{\pi T^2 \mu}{v_g^2} = 2P_L^T, \quad (37)$$

so we need to keep finite temperature corrections in the leads as well.

In our sample, the situation is more involved since in neutral graphene the electric current is not related to the hydrodynamic velocity. As a manifestation of this fact, the differential equations (10) and (11) decouple into two disjunct sets. The first one consists of equations (10a) and (11a) with the solution

$$\delta j_r = \frac{I}{2\pi e r}, \quad (38)$$

$$E_r = \frac{IR_0}{2\pi r}, \quad \phi = -\frac{IR_0}{2\pi} \log\left(\frac{r}{r_0}\right). \quad (39)$$

The constant r_0 (not necessarily the same as in the corresponding solution for the leads) is not fixed by the boundary conditions we have imposed so far.

The second set of equations consists of (10b), (10d), (10e) and (11c). Expressing δP through u_r , we find

$$0 = \partial_r \left(\frac{1}{r} \frac{\partial(r u_r)}{\partial r} \right) - \frac{u_r}{\ell_{\text{GE}}^2} \quad (40)$$

$$\frac{1}{\ell_{\text{GE}}^2} = \left(\eta + \frac{3P\tau_{RE}}{2} \right)^{-1} \frac{3P}{v_g^2 \tau_{\text{dis}}}, \quad (41)$$

where the Gurzhi length is renormalized by energy relaxation through the combination $\eta' = \eta + 3P\tau_{RE}/2$. The other two equations can be combined to form

$$\partial_r \left(\frac{1}{r} \frac{\partial(r u_r)}{\partial r} \right) - M \partial_r \left(\frac{1}{r} \frac{\partial(r \frac{\partial \mu_I}{\partial r})}{\partial r} \right) = - \frac{M}{\ell_R^2} \frac{\partial \mu_I(r)}{\partial r} \quad (42)$$

$$M = \frac{2T \ln 2}{n_{I,0} \pi} \frac{\delta_I}{\tau_{\text{dis}}^{-1} + \delta_I^{-1} \tau_{22}^{-1}}, \quad \ell_R^2 = \frac{\delta_I}{\tau_{\text{dis}}^{-1} + \delta_I^{-1} \tau_{22}^{-1}} \frac{\pi T^2 \tau_R}{6n_{I,0}}. \quad (43)$$

The two coupled Bessel differential equations for u_r and $\partial_r \mu_I$ can be expressed using the differential operator $\mathbb{D} = \partial_r(1/r)\partial_r r$. This way we can write the system of equations in the matrix form

$$\mathbb{D} \begin{pmatrix} 1 & 0 \\ 1 & -M \end{pmatrix} \begin{pmatrix} u_r \\ \frac{\partial \mu_I}{\partial r} \end{pmatrix} = \begin{pmatrix} \frac{1}{\ell_{\text{GE}}^2} & 0 \\ 0 & -\frac{M}{\ell_R^2} \end{pmatrix} \begin{pmatrix} u_r \\ \frac{\partial \mu_I}{\partial r} \end{pmatrix} \Leftrightarrow \mathbb{D} \begin{pmatrix} u_r \\ \frac{\partial \mu_I}{\partial r} \end{pmatrix} = \begin{pmatrix} \frac{1}{\ell_{\text{GE}}^2} & 0 \\ \frac{1}{M\ell_{\text{GE}}^2} & \frac{1}{\ell_R^2} \end{pmatrix} \begin{pmatrix} u_r \\ \frac{\partial \mu_I}{\partial r} \end{pmatrix}. \quad (44)$$

This can be formally solved by diagonalizing the matrix

$$\begin{pmatrix} \frac{1}{\ell_{\text{GE}}^2} & 0 \\ \frac{1}{M\ell_{\text{GE}}^2} & \frac{1}{\ell_R^2} \end{pmatrix} = \hat{U}^{-1} \hat{D} \hat{U}, \quad (45)$$

where \hat{D} is a diagonal matrix with the eigenvalues d_1 and d_2 (in units of inverse length squared) and then transforming back to the u_r and $\partial_r \mu_I$ basis. Then this coupled Bessel differential equation has the general solution

$$u_r = M \left(1 - \frac{\ell_{\text{GE}}^2}{\ell_R^2} \right) \left[f_1 I_1 \left(\frac{r}{\ell_{\text{GE}}} \right) + f_2 K_1 \left(\frac{r}{\ell_{\text{GE}}} \right) \right] \quad (46)$$

$$\frac{\partial \mu_I}{\partial r} = f_1 I_1 \left(\frac{r}{\ell_{\text{GE}}} \right) + f_2 K_1 \left(\frac{r}{\ell_{\text{GE}}} \right) + g_1 I_1 \left(\frac{r}{\ell_R} \right) + g_2 K_1 \left(\frac{r}{\ell_R} \right), \quad (47)$$

where the coefficients f_1 , f_2 , g_1 and g_2 should be determined from the boundary conditions. These involve the entropy density

$$T s_B = 3P = 3 \frac{3T^3 \zeta(3)}{\pi v_g^2}. \quad (48)$$

From the conservation of entropy current Eqs. (26) and (29) we find f_1 and f_2 so that

$$u_r = \frac{I_{SL}}{2\pi e n_{LSB}} \left\{ \frac{I_1 \left(\frac{r}{\ell_{\text{GE}}} \right) \left[r_1 K_1 \left(\frac{r_1}{\ell_{\text{GE}}} \right) - r_2 K_1 \left(\frac{r_2}{\ell_{\text{GE}}} \right) \right] - K_1 \left(\frac{r}{\ell_{\text{GE}}} \right) \left[r_1 I_1 \left(\frac{r_1}{\ell_{\text{GE}}} \right) - r_2 I_1 \left(\frac{r_2}{\ell_{\text{GE}}} \right) \right]}{r_1 r_2 K_1 \left(\frac{r_1}{\ell_{\text{GE}}} \right) I_1 \left(\frac{r_2}{\ell_{\text{GE}}} \right) - r_1 r_2 I_1 \left(\frac{r_1}{\ell_{\text{GE}}} \right) K_1 \left(\frac{r_2}{\ell_{\text{GE}}} \right)} \right\}. \quad (49)$$

This leads to the stress tensor elements

$$\sigma_{rr} = \frac{\eta I_{SL}}{2\pi e \ell_{\text{GENLSB}}} \frac{I_2 \left(\frac{r}{\ell_{\text{GE}}} \right) \left[r_1 K_1 \left(\frac{r_1}{\ell_{\text{GE}}} \right) - r_2 K_1 \left(\frac{r_2}{\ell_{\text{GE}}} \right) \right] + K_2 \left(\frac{r}{\ell_{\text{GE}}} \right) \left[r_1 I_1 \left(\frac{r_1}{\ell_{\text{GE}}} \right) - r_2 I_1 \left(\frac{r_2}{\ell_{\text{GE}}} \right) \right]}{r_1 r_2 \left[K_1 \left(\frac{r_1}{\ell_{\text{GE}}} \right) I_1 \left(\frac{r_2}{\ell_{\text{GE}}} \right) - I_1 \left(\frac{r_1}{\ell_{\text{GE}}} \right) K_1 \left(\frac{r_2}{\ell_{\text{GE}}} \right) \right]}, \quad (50)$$

$$\sigma_{r\vartheta} = 0 \quad (51)$$

and

$$\begin{aligned} \delta P &= -\frac{3P\tau_{\text{RE}}}{2} \frac{1}{r} \frac{\partial(ru_r)}{\partial r} = \\ &= -\frac{3P\tau_{\text{RE}}}{2} \frac{I_{S_L}}{2\pi\epsilon\ell_{\text{GE}}n_Ls_B} \left[\frac{K_0\left(\frac{r}{\ell_{\text{GE}}}\right) \left[r_1 I_1\left(\frac{r_1}{\ell_{\text{GE}}}\right) - r_2 I_1\left(\frac{r_2}{\ell_{\text{GE}}}\right) \right] + I_0\left(\frac{r}{\ell_{\text{GE}}}\right) \left[r_1 K_1\left(\frac{r_1}{\ell_{\text{GE}}}\right) - r_2 K_1\left(\frac{r_2}{\ell_{\text{GE}}}\right) \right]}{r_1 r_2 K_1\left(\frac{r_1}{\ell_{\text{GE}}}\right) I_1\left(\frac{r_2}{\ell_{\text{GE}}}\right) - r_1 r_2 I_1\left(\frac{r_1}{\ell_{\text{GE}}}\right) K_1\left(\frac{r_2}{\ell_{\text{GE}}}\right)} \right], \end{aligned} \quad (52)$$

Using the conservation of the imbalance current Eqs. (25) and (28) we find the imbalance chemical potential

$$\begin{aligned} \mu_I(r) &= \frac{I_{S_L}\ell_R}{2\pi\epsilon Mn_L r_1 r_2 s_B (\ell_{\text{GE}}^2 - \ell_R^2)} \left[\frac{K_0\left(\frac{r}{\ell_R}\right) \left[r_1 I_1\left(\frac{r_1}{\ell_R}\right) - r_2 I_1\left(\frac{r_2}{\ell_R}\right) \right] \left[\ell_{\text{GE}}^2 + (\ell_R^2 - \ell_{\text{GE}}^2) \frac{n_L s_B}{n_{I,0} s_L} \right]}{K_1\left(\frac{r_1}{\ell_R}\right) I_1\left(\frac{r_2}{\ell_R}\right) - I_1\left(\frac{r_1}{\ell_R}\right) K_1\left(\frac{r_2}{\ell_R}\right)} \right. \\ &+ \frac{I_0\left(\frac{r}{\ell_R}\right) \left[r_1 K_1\left(\frac{r_1}{\ell_R}\right) - r_2 K_1\left(\frac{r_2}{\ell_R}\right) \right] \left[\ell_{\text{GE}}^2 + (\ell_R^2 - \ell_{\text{GE}}^2) \frac{n_L s_B}{n_{I,0} s_L} \right]}{K_1\left(\frac{r_1}{\ell_R}\right) I_1\left(\frac{r_2}{\ell_R}\right) - I_1\left(\frac{r_1}{\ell_R}\right) K_1\left(\frac{r_2}{\ell_R}\right)} \\ &+ \left. \frac{\ell_{\text{GE}}\ell_R K_0\left(\frac{r}{\ell_{\text{GE}}}\right) \left[r_2 I_1\left(\frac{r_2}{\ell_{\text{GE}}}\right) - r_1 I_1\left(\frac{r_1}{\ell_{\text{GE}}}\right) \right] + \ell_{\text{GE}}\ell_R I_0\left(\frac{r}{\ell_{\text{GE}}}\right) \left[r_2 K_1\left(\frac{r_2}{\ell_{\text{GE}}}\right) - r_1 K_1\left(\frac{r_1}{\ell_{\text{GE}}}\right) \right]}{K_1\left(\frac{r_1}{\ell_{\text{GE}}}\right) I_1\left(\frac{r_2}{\ell_{\text{GE}}}\right) - I_1\left(\frac{r_1}{\ell_{\text{GE}}}\right) K_1\left(\frac{r_2}{\ell_{\text{GE}}}\right)} + \frac{\ell_{\text{GE}}\ell_R I_0\left(\frac{r}{\ell_{\text{GE}}}\right) \left[r_2 K_1\left(\frac{r_2}{\ell_{\text{GE}}}\right) - r_1 K_1\left(\frac{r_1}{\ell_{\text{GE}}}\right) \right]}{K_1\left(\frac{r_1}{\ell_{\text{GE}}}\right) I_1\left(\frac{r_2}{\ell_{\text{GE}}}\right) - I_1\left(\frac{r_1}{\ell_{\text{GE}}}\right) K_1\left(\frac{r_2}{\ell_{\text{GE}}}\right)} \right] \end{aligned} \quad (53)$$

and the dissipative correction to the imbalance current

$$\begin{aligned} \delta j_{I_r}(r) &= \frac{In_{I,0}s_L}{2\pi\epsilon n_L r_1 r_2 s_B (\ell_{\text{GE}}^2 - \ell_R^2)} \left[\frac{K_1\left(\frac{r}{\ell_R}\right) \left[r_1 I_1\left(\frac{r_1}{\ell_R}\right) - r_2 I_1\left(\frac{r_2}{\ell_R}\right) \right] \left[\ell_{\text{GE}}^2 + (\ell_R^2 - \ell_{\text{GE}}^2) \frac{n_L s_B}{n_{I,0} s_L} \right]}{K_1\left(\frac{r_1}{\ell_R}\right) I_1\left(\frac{r_2}{\ell_R}\right) - I_1\left(\frac{r_1}{\ell_R}\right) K_1\left(\frac{r_2}{\ell_R}\right)} \right. \\ &- \frac{I_1\left(\frac{r}{\ell_R}\right) \left[r_1 K_1\left(\frac{r_1}{\ell_R}\right) - r_2 K_1\left(\frac{r_2}{\ell_R}\right) \right] \left[\ell_{\text{GE}}^2 + (\ell_R^2 - \ell_{\text{GE}}^2) \frac{n_L s_B}{n_{I,0} s_L} \right]}{K_1\left(\frac{r_1}{\ell_R}\right) I_1\left(\frac{r_2}{\ell_R}\right) - I_1\left(\frac{r_1}{\ell_R}\right) K_1\left(\frac{r_2}{\ell_R}\right)} \\ &+ \left. \frac{\ell_R^2 K_1\left(\frac{r}{\ell_{\text{GE}}}\right) \left[r_1 I_1\left(\frac{r_1}{\ell_{\text{GE}}}\right) - r_2 I_1\left(\frac{r_2}{\ell_{\text{GE}}}\right) \right]}{K_1\left(\frac{r_1}{\ell_{\text{GE}}}\right) I_1\left(\frac{r_2}{\ell_{\text{GE}}}\right) - I_1\left(\frac{r_1}{\ell_{\text{GE}}}\right) K_1\left(\frac{r_2}{\ell_{\text{GE}}}\right)} + \frac{\ell_R^2 I_1\left(\frac{r}{\ell_{\text{GE}}}\right) \left[r_2 K_1\left(\frac{r_2}{\ell_{\text{GE}}}\right) - r_1 K_1\left(\frac{r_1}{\ell_{\text{GE}}}\right) \right]}{K_1\left(\frac{r_1}{\ell_{\text{GE}}}\right) I_1\left(\frac{r_2}{\ell_{\text{GE}}}\right) - I_1\left(\frac{r_1}{\ell_{\text{GE}}}\right) K_1\left(\frac{r_2}{\ell_{\text{GE}}}\right)} \right]. \end{aligned} \quad (54)$$

From δP and μ_I we find δT according to

$$\delta T = \frac{\pi v_g^2}{9T^2\zeta(3)} \delta P - \frac{\pi^2}{27\zeta(3)} \mu_I. \quad (55)$$

Our hydrodynamic system is not characterized by a local thermal conductivity κ . In other words, the heat current

$$\vec{j}_Q(r) = 3P\vec{u} - \mu\vec{j} - \mu_I\vec{j}_I \quad (56)$$

is related to the temperature gradient $\nabla\delta T(r)$ at the same point r non locally. The non-local (integral) relation between $\vec{j}_Q(r)$ and $\nabla\delta T(r')$ characterized by a non-local kernel $\kappa(r, r')$ follows from the fact that the equation for $\vec{u}(r)$ is now a second-order differential equation with a non-local Green's function. Expressing $\delta P(r)$ there in terms of $\delta T(r)$ and $\mu_I(r)$, we have a non-local relation between $\vec{u}(r)$, $\delta T(r')$ and $\nabla\mu_I(r')$. Substituting this $\vec{u}(r)$ into the definition of $\vec{j}_Q(r)$, we obtain a non-local thermal conductivity. As a result one can only introduce the thermal conductance for the device, relating the temperature difference between the contacts with the total heat current through the system. This will be done in a subsequent publication.

Dissipation and total resistance

The above solution is not sufficient to determine the drop in electrochemical potential between the points r_{in} and r_{out} (in the inner and outer lead, respectively) since it contains the undefined constant r_0 that has to be determined from a boundary condition for the electric potential. Although microscopically the potential has to be continuous, several

effects might contribute to an apparent discontinuity on the hydrodynamic scale. The most obvious contribution is the contact resistance that is a manifestation of the different work functions in the two materials across the interface as well as the mismatch in their chemical potentials [65]. A more subtle effect due to electron-electron interaction giving rise to viscosity and hence an additional dissipation channel [66]. At charge neutrality, this effect is subtle, since the electric current is decoupled from the hydrodynamic energy flow. However, both flows are induced by the same current source providing the energy dissipated by means of both the Ohmic and viscous effects [66] as well as energy relaxation [48]. The latter processes should be taken into account in the form of an additional voltage drop at the interface.

Under the assumption that energy is not being accumulated at the interface, we generalize the idea proposed in Ref. [66] and consider viscous dissipation in the sample. Since the electric field in bulk of the sample is completely determined by the Ohmic resistance R_0 , additional dissipation due to viscosity and energy relaxation corresponds to a jump in the electric potential (on the hydrodynamic scale) at the interface. Microscopically, the voltage jump is due to an excess electric field in the Knudsen layer around the sample-lead boundary.

Consider the kinetic energy associated with the hydrodynamic flow that can be found from the energy density

$$\mathcal{E} = \int dV (n_E - n_E(\vec{u} = 0)) \approx \int dV \frac{6P}{v_g^2} \vec{u}^2. \quad (57)$$

Working within linear response, here we only keep terms up to the second order in \vec{u} (and thus the drive I). Dissipation is then describe by

$$\mathcal{A} = \dot{\mathcal{E}} = 2 \frac{6P}{v_g^2} \int dV \vec{u} \partial_t \vec{u} = 0, \quad (58)$$

vanishing in the steady state. This expression can now be simplified using the generalized Navier-Stokes equation.

In the leads (still assuming graphene at finite carrier density) we find

$$\begin{aligned} \frac{3P_L}{v_g^2} \vec{u}_L \partial_t \vec{u}_L &= \vec{u}_L \left(-\frac{3P_L}{v_g^2} \frac{\vec{u}_L}{\tau_L} - \vec{\nabla} \check{\Pi}_E + n_L e \vec{E} \right) \\ &= -\frac{3P_L}{v_g^2} \frac{\vec{u}_L^2}{\tau_L} - \vec{\nabla} \delta P \vec{u}_L + \vec{u}_L \vec{\nabla} \check{\sigma} - e \vec{j} \vec{\nabla} \phi. \\ &= -\frac{3P_L}{v_g^2} \frac{\vec{u}_L^2}{\tau_L} - \frac{\partial u_{L,i}}{\partial x_j} \sigma_{ij} + \vec{\nabla} \left(\vec{u}_L \check{\sigma} - e \vec{j} \phi - \vec{u}_L \delta P \right). \end{aligned} \quad (59)$$

The term $en_L \vec{u}_L \vec{E} = e \vec{j} \vec{E}$ is the Joule heating. Using the divergence theorem we can divide this into a boundary and a bulk term

$$0 = \mathcal{A} = \mathcal{A}_{\text{boundary}} - \mathcal{A}_{\text{bulk}}, \quad (60)$$

$$\mathcal{A}_{\text{boundary}} = 4 \int d\vec{A} \left(\vec{u}_L \check{\sigma} - \vec{u}_L \delta P - e \vec{j} \phi \right), \quad (61)$$

$$\mathcal{A}_{\text{bulk}} = 4 \int dV \left(\frac{3P_L}{v_g^2} \frac{\vec{u}_L^2}{\tau_L} + \frac{\partial u_{L,i}}{\partial x_j} \sigma_{ij} \right). \quad (62)$$

The boundary term includes the energy transmitted through the interface.

Since the current density is conserved at the interface, we can immediately write down the corresponding equation in the neutral graphene sample, where the Joule heating is given by $e \delta \vec{j} \vec{E}$. Then we find

$$0 = \mathcal{A} = \mathcal{A}_{\text{boundary}} - \mathcal{A}_{\text{bulk}}, \quad (63)$$

$$\mathcal{A}_{\text{boundary}} = 4 \int d\vec{A} \left(\vec{u} \sigma - \vec{u} \delta P - e \delta \vec{j} \phi \right), \quad (64)$$

$$\mathcal{A}_{\text{bulk}} = 4 \int dV \left(\frac{3P}{v_g^2} \frac{\vec{u}^2}{\tau_{\text{dis}}} + \frac{\partial u_i}{\partial x_j} \sigma_{ij} - \delta P (\vec{\nabla} \cdot \vec{u}) \right). \quad (65)$$

As stated above, under realistic experimental conditions the non-equilibrium part of the pressure at $u = 0$ on the lead side vanishes

$$\delta P = 0. \quad (66)$$

At the same time, in neutral graphene sample we find

$$\delta P = \left(\frac{9T^2 \delta T \zeta(3)}{\pi v_g^2} + \frac{\pi \mu_I T^2}{3v_g^2} \right) = \frac{T^2}{v_g^2} \left(\frac{9\delta T \zeta(3)}{\pi} + \frac{\pi \mu_I}{3} \right). \quad (67)$$

Using the hydrodynamic equations, one may replace δP by $[-3P_B \tau_{RE}/(2r)]\partial(ru_r)/\partial r$, thus determining δP for finite τ_{RE} without any additional boundary conditions. The same goes for μ_I . Thus we may use the viscous part of the dissipation to find the difference in the electrochemical potential across the interface.

In addition, we may include the contact resistance described by

$$I^2 R_c = \vec{I}^T \check{R} \vec{I}, \quad (68)$$

where \vec{I} includes charge and entropy current and \check{R} includes the thermoelectric coefficients of the interface.

In the absence of magnetic field, both u_ϑ and $\sigma_{r\vartheta}$ vanish. In the leads $\delta P = 0$ and hence we find the condition

$$\begin{aligned} 4\pi [r(u_r \sigma_{rr})]_{r_1-\epsilon} - 2I\phi(r_1 - \epsilon) &= 4\pi [r(u_r \sigma_{rr} - u_r \delta P)]_{r_1+\epsilon} - 2I\phi(r_1 + \epsilon) - 2\vec{I}^T \check{R} \vec{I} \\ \Leftrightarrow \phi(r_1 - \epsilon) - \phi(r_1 + \epsilon) &= \frac{2\pi}{I} \{ [r(u_r \sigma_{rr})]_{r_1-\epsilon} - [r(u_r \sigma_{rr} - u_r \delta P)]_{r_1+\epsilon} \} + IR_c \end{aligned} \quad (69)$$

at the first interface and similarly for the second interface

$$\begin{aligned} 4\pi [r(u_r \sigma_{rr} - \delta P u_r)]_{r_2-\epsilon} - 2I\phi(r_2 - \epsilon) &= 4\pi [r(u_r \sigma_{rr})]_{r_2+\epsilon} - 2I\phi(r_2 + \epsilon) - 2\vec{I}^T \check{R} \vec{I} \\ \Leftrightarrow \phi(r_2 - \epsilon) - \phi(r_2 + \epsilon) &= -\frac{2\pi}{I} \{ [r(u_r \sigma_{rr})]_{r_2+\epsilon} - [r(u_r \sigma_{rr} - u_r \delta P)]_{r_2-\epsilon} \} + IR_c. \end{aligned} \quad (70)$$

Combining the above general solution with these conditions, we find at r_1

$$ru_r(\sigma_{rr} - \delta P) = \frac{I^2 s_L^2 \eta \ell_{GE}}{4\pi^2 e^2 n_L^2 s_B^2 \ell_G^2} \frac{\ell_{GE} - r_2 K_0\left(\frac{r_1}{\ell_{GE}}\right) I_1\left(\frac{r_2}{\ell_{GE}}\right) - r_2 I_0\left(\frac{r_1}{\ell_{GE}}\right) K_1\left(\frac{r_2}{\ell_{GE}}\right)}{r_1 r_2 \left[K_1\left(\frac{r_1}{\ell_{GE}}\right) I_1\left(\frac{r_2}{\ell_{GE}}\right) - I_1\left(\frac{r_1}{\ell_{GE}}\right) K_1\left(\frac{r_2}{\ell_{GE}}\right) \right]} - \frac{\eta I^2 s_L^2}{2\pi^2 e^2 n_L^2 r_1^2 s_B^2}$$

and at r_2

$$ru_r(\sigma_{rr} - \delta P) = -\frac{I^2 s_L^2 \eta \ell_{GE}}{4\pi^2 e^2 \ell_G^2 n_L^2 s_B^2} \frac{\ell_{GE} - r_1 I_1\left(\frac{r_1}{\ell_{GE}}\right) K_0\left(\frac{r_2}{\ell_{GE}}\right) - r_1 K_1\left(\frac{r_1}{\ell_{GE}}\right) I_0\left(\frac{r_2}{\ell_{GE}}\right)}{r_1 r_2 \left[K_1\left(\frac{r_1}{\ell_{GE}}\right) I_1\left(\frac{r_2}{\ell_{GE}}\right) - I_1\left(\frac{r_1}{\ell_{GE}}\right) K_1\left(\frac{r_2}{\ell_{GE}}\right) \right]} - \frac{\eta I^2 s_L^2}{2\pi^2 e^2 n_L^2 r_2^2 s_B^2}.$$

As a result, we find the total resistance R of the system in the form

$$IR = \phi(r_{in}) - \phi(r_{out}) = I(R_L + R_B + 2R_C + R_L^{\text{diss}} + R_B^{\text{diss}}), \quad (71)$$

$$R_L = \frac{3P_L}{2\pi e^2 n_L^2 v_g^2 \tau_L} \log\left(\frac{r_1 r_{out}}{r_{in} r_2}\right), \quad R_B = \frac{R_0}{2\pi} \log\left(\frac{r_2}{r_1}\right), \quad (72)$$

$$R_C = \frac{\vec{I}^T \check{R} \vec{I}}{I^2}, \quad (73)$$

$$R_L^{\text{diss}} = \frac{\eta L}{\pi e^2 n_L^2} \left(\frac{1}{r_2^2} - \frac{1}{r_1^2} \right) \quad (74)$$

$$\begin{aligned} R_B^{\text{diss}} &= \frac{\eta s_L^2}{\pi e^2 n_L^2 s_B^2} \left\{ \frac{1}{r_1^2} - \frac{1}{r_2^2} + \frac{\ell_{GE}}{2\ell_G^2} \right. \\ &\times \left. \frac{r_2 \left[K_0\left(\frac{r_1}{\ell_{GE}}\right) I_1\left(\frac{r_2}{\ell_{GE}}\right) + I_0\left(\frac{r_1}{\ell_{GE}}\right) K_1\left(\frac{r_2}{\ell_{GE}}\right) \right] + r_1 \left[I_1\left(\frac{r_1}{\ell_{GE}}\right) K_0\left(\frac{r_2}{\ell_{GE}}\right) + K_1\left(\frac{r_1}{\ell_{GE}}\right) I_0\left(\frac{r_2}{\ell_{GE}}\right) \right] - 2\ell_{GE}}{r_1 r_2 \left(K_1\left(\frac{r_1}{\ell_{GE}}\right) I_1\left(\frac{r_2}{\ell_{GE}}\right) - I_1\left(\frac{r_1}{\ell_{GE}}\right) K_1\left(\frac{r_2}{\ell_{GE}}\right) \right)} \right\}. \end{aligned} \quad (75)$$

Analysis of results

The behavior of the obtained resistance depends on the hierarchy of length scales r_1 , r_2 , $r_2 - r_1$, ℓ_{GE} and ℓ_R . In this Section, we specify the quantitative values of the parameters used to produce the plots shown in the main text. For clarity, here we restore the constants \hbar and k_B .

We perform our quantitative analysis assuming the carrier density in the leads to be $n_L = 5 \times 10^{14} \text{ m}^{-2}$. The equilibrium temperature in the device (including both leads and the sample) is fixed to $T = 100 \text{ K}$. The current, that is supplied by the source is $I = 1 \mu\text{A}$ and we assume that the effective interaction constant is screened to $\alpha = 0.2$. We further use $\tau_{\text{dis}} = 1.25 \times 10^{-12} \text{ s}$ and $\tau_L = 0.189 \times 10^{-12} \text{ s}$ [65], since the density is higher in the leads. This determines all other parameters, except for τ_{RE} and τ_R (or alternatively ℓ_{GE} and ℓ_R). Since these quantities are difficult to extract from the available experimental data, we show results for several different regimes.

The time scales related to electron-electron interaction are given by [63]

$$\tau_{ii} = \hbar \frac{4\pi t_{ii} \log 2}{\alpha^2 k_B T}, \quad t_{11} = \frac{1}{33.13}, \quad t_{22} = \frac{1}{5.45}. \quad (76)$$

For the above parameter values, we find $\tau_{11} = 0.5 \times 10^{-12} \text{ s}$ and $\tau_{22} = 3 \times 10^{-12} \text{ s}$. The viscosity can be estimated as

$$\eta = \frac{0.446 k_B^2 T^2}{\alpha^2 v_g^2 \hbar} \quad (77)$$

and amounts to $\nu = v_g^2 \eta / (3P) = 0.25 \text{ m}^2/\text{s}$. In addition

$$R_0 = \frac{\pi}{2 \log 2} \frac{\hbar^2}{e^2 k_B T} \left(\frac{1}{\tau_{11}} + \frac{1}{\tau_{\text{dis}}} \right) = 1985.33 \Omega \quad (78)$$

When describing the hydrodynamic velocity u_r and the pressure δP one can consider three different limits. If $\ell_{\text{GE}} \ll r_1, r_2$, which is achieved for very small τ_{dis} , one finds

$$u_r \approx \frac{I s_L \left(\sqrt{r r_2} \sinh \left(\frac{r-r_2}{\ell_{\text{GE}}} \right) - \sqrt{r r_1} \sinh \left(\frac{r-r_1}{\ell_{\text{GE}}} \right) \right)}{2\pi e n_L r s_B \sqrt{r_1 r_2} \sinh \left(\frac{r_1-r_2}{\ell_{\text{GE}}} \right)} \quad (79)$$

which means, that the velocity vanishes exponentially close to the interface and is very small in the bulk of the sample. In the opposite limit $\ell_{\text{GE}} \gg r_1, r_2$ u_r shows a behavior similar to the drift velocity in the leads with logarithmic corrections

$$u_r \approx \frac{I s_L}{2\pi e n_L r s_B} + \frac{I s_L r_1^2 r_2^2 \log \left(\frac{r_1}{r_2} \right)}{4\pi e \ell_{\text{GE}}^2 n_L r s_B (r_1^2 - r_2^2)} + \frac{I r s_L \left[r_1^2 \log \left(\frac{r}{r_1} \right) - r_2^2 \log \left(\frac{r}{r_2} \right) \right]}{4\pi e \ell_{\text{GE}}^2 n_L s_B (r_1^2 - r_2^2)}. \quad (80)$$

Finally, if $r_2 - r_1 \ll r_1, r_2, \ell_{\text{GE}}$ we find the same $1/r$ behavior as in the leads

$$u_r \approx \frac{I s_L}{2\pi e n_L r s_B} \quad (81)$$

The resulting velocity u_r is shown in Fig. 2 of the main text. In the leads, the drift velocity shows a simple $1/r$ behavior, while one finds a jump due to the mismatch of entropy directly at the interface. Inside the sample, the situation depends on the relative size of ℓ_{GE} . If $\ell_{\text{GE}} \ll r_1, r_2$ we indeed observe, that the velocity decreases rapidly close to the interface and exactly vanishes in the bulk of the sample. This behavior is generally only observable in rather large samples, since the quantity τ_{dis} cannot be arbitrarily small while still staying in the hydrodynamic regime. In all other cases, u_r resembles a $1/r$ behavior, that is slightly modified by logarithmic corrections.

The plot of δT are shown in Fig. 3 of the main text. In the limit of $\ell_{\text{GE}} \ll r_1, r_2$ the non-equilibrium part of the temperature δT vanishes in the bulk of the sample. In this limit energy relaxation processes transfer any heating, that may develop in the sample to the substrate and out of the device. There is only a small finite effect very close to the interface. Since this is an effect of τ_R it is in principle independent of ℓ_{GE} and τ_{RE} , however we need $\ell_R < \ell_{\text{GE}}$ to remain in the hydrodynamic regime. In all other scenarios, there is a finite temperature profile, which may amount to 0.5% of the equilibrium temperature.

Finally we take a look at the total resistance R of the system. In general one might place the measuring points r_{in} and r_{out} very close to the interface, in which case the bulk resistance of the leads R_L would not contribute to the total resistance R . We will further disregard the influence of the phenomenological contact resistance R_C , which only depends on the used materials and their relative chemical potential. Then one can consider again three limiting cases

of the hydrodynamic, dissipative contribution to the resistance R_B^{diss} . The first limit is $\ell_{\text{GE}} \ll r_1, r_2$ in which case we find

$$R_B^{\text{diss}} \approx \frac{\eta s_L^2}{\pi e^2 n_L^2 s_B^2} \left(\frac{1}{r_1^2} - \frac{1}{r_2^2} \right) - \frac{s_L^2 (A + \eta) \left((r_1 + r_2) \cosh \left(\frac{r_1 - r_2}{\ell_{\text{GE}}} \right) - 2\sqrt{r_1 r_2} \right) \text{csch} \left(\frac{r_1 - r_2}{\ell_{\text{GE}}} \right)}{2\pi e^2 \ell_{\text{GE}} n_L^2 r_1 r_2 s_B^2} \quad (82)$$

$$\approx \frac{\eta s_L^2}{\pi e^2 n_L^2 s_B^2} \left[\frac{1}{r_1^2} - \frac{1}{r_2^2} - \frac{\sqrt{\ell_G^2 + \frac{v_g^2 \tau_{\text{dis}} \tau_{\text{RE}}}{2}}}{2\ell_G^2} \left(\frac{1}{r_1} + \frac{1}{r_2} \right) \right] \quad (83)$$

where the second approximation requires $r_1 - r_2 \gg \ell_{\text{GE}}$. The result of Ref. [66] corresponds to neglecting the term proportional to ℓ_{GE} . The second limit is the case $\ell_{\text{GE}} \gg r_1, r_2$ and we find

$$R_B^{\text{diss}} \approx \frac{\eta s_L^2}{\pi e^2 n_L^2 s_B^2} \left(\frac{1}{r_1^2} - \frac{1}{r_2^2} + \frac{1}{2\ell_G^2} \log \left(\frac{r_2}{r_1} \right) \right), \quad (84)$$

which introduces a logarithmic correction of exactly the same form as the bulk resistance R_B of the sample. The final limit is $r_2 - r_1 \ll r_1, r_2, \ell_{\text{GE}}$ where we find the result

$$R_B^{\text{diss}} = \frac{s_L^2 \eta (r_2^2 - r_1^2)}{4\pi e^2 n_L^2 r_1 r_2 s_B^2 \ell_G^2}. \quad (85)$$

If one instead directly takes the limit $\tau_{\text{RE}} \rightarrow 0$, and additionally $\ell_G \ll r_1, r_2, r_2 - r_1$ one would obtain

$$R_B^{\text{diss}} \approx \frac{\eta s_L^2}{\pi e^2 n_L^2 s_B^2} \left[\frac{1}{r_1^2} - \frac{1}{r_2^2} - \frac{1}{2\ell_G} \left(\frac{1}{r_1} + \frac{1}{r_2} \right) \right]. \quad (86)$$

This is the result for the viscous correction to the resistance at charge neutrality in the setup of Ref. [67].

The plots for $\phi(r)$ and $R = R_B + R_B^{\text{diss}} + R_L^{\text{diss}}$ are shown in Fig. 4 and 5 of the main text respectively. In the case of the potential ϕ we find a logarithmic dependence on the radial position r in both the leads and the sample, where the overall prefactor is however different. In all considered cases, the jump at the interface is in the same direction, which for the second interface is opposite to what Ref. [66] obtains. This is due to the fact, that in our case the contribution of δP is larger than the contributions due to η and η_L alone. The jump is larger, for larger ℓ_{GE} . As seen in Fig. 5 of the main text, the total measured resistance is only slightly changed. The correction shown in the inset of Fig. 5 of the main text is nearly logarithmic for the larger ℓ_{GE} , while saturates for the smaller ℓ_{GE} .

-
- [1] J. M. Ziman, *Principles of the Theory of Solids* (Cambridge University Press, Cambridge, 1965).
 - [2] D. A. Bandurin, I. Torre, R. Krishna Kumar, M. Ben Shalom, A. Tomadin, A. Principi, G. H. Auton, E. Khestanova, K. S. Novoselov, I. V. Grigorieva, et al., *Science* **351**, 1055 (2016).
 - [3] J. Crossno, J. K. Shi, K. Wang, X. Liu, A. Harzheim, A. Lucas, S. Sachdev, P. Kim, T. Taniguchi, K. Watanabe, et al., *Science* **351**, 1058 (2016).
 - [4] R. Krishna Kumar, D. A. Bandurin, F. M. D. Pellegrino, Y. Cao, A. Principi, H. Guo, G. H. Auton, M. Ben Shalom, L. A. Ponomarenko, G. Falkovich, et al., *Nat. Phys.* **13**, 1182 (2017).
 - [5] F. Ghahari, H.-Y. Xie, T. Taniguchi, K. Watanabe, M. S. Foster, and P. Kim, *Phys. Rev. Lett.* **116**, 136802 (2016).
 - [6] D. A. Bandurin, A. V. Shytov, L. S. Levitov, R. Krishna Kumar, A. I. Berdyugin, M. Ben Shalom, I. V. Grigorieva, A. K. Geim, and G. Falkovich, *Nat. Commun.* **9**, 4533 (2018).
 - [7] A. I. Berdyugin, S. G. Xu, F. M. D. Pellegrino, R. Krishna Kumar, A. Principi, I. Torre, M. B. Shalom, T. Taniguchi, K. Watanabe, I. V. Grigorieva, et al., *Science* **364**, 162 (2019).
 - [8] P. Gallagher, C.-S. Yang, T. Lyu, F. Tian, R. Kou, H. Zhang, K. Watanabe, T. Taniguchi, and F. Wang, *Science* **364**, 158 (2019).
 - [9] M. J. H. Ku, T. X. Zhou, Q. Li, Y. J. Shin, J. K. Shi, C. Burch, L. E. Anderson, A. T. Pierce, Y. Xie, A. Hamo, et al., *Nature* **583**, 537 (2020).
 - [10] J. A. Sulpizio, L. Ella, A. Rozen, J. Birkbeck, D. J. Perello, D. Dutta, M. Ben-Shalom, T. Taniguchi, K. Watanabe, T. Holder, et al., *Nature* **576**, 75 (2019).
 - [11] A. Jenkins, S. Baumann, H. Zhou, S. A. Meynell, D. Yang, T. T. K. Watanabe, A. Lucas, A. F. Young, and A. C. Bleszynski Jayich (2020), arXiv:2002.05065.

- [12] P. J. W. Moll, P. Kushwaha, N. Nandi, B. Schmidt, and A. P. Mackenzie, *Science* **351**, 1061 (2016).
- [13] B. A. Braem, F. M. D. Pellegrino, A. Principi, M. Rösli, C. Gold, S. Hennel, J. V. Koski, M. Berl, W. Dietsche, W. Wegscheider, et al., *Phys. Rev. B* **98**, 241304(R) (2018).
- [14] A. Jaoui, B. Fauqué, C. W. Rischau, A. Subedi, C. Fu, J. Gooth, N. Kumar, V. Süß, D. L. Maslov, C. Felser, et al., *npj Quantum Materials* **3**, 64 (2018).
- [15] M. S. Steinberg, *Phys. Rev.* **109**, 1486 (1958).
- [16] R. N. Gurzhi, *Soviet Physics Uspekhi* **11**, 255 (1968), [*Usp. Fiz. Nauk* **94**, 689 (1968)].
- [17] B. Bradlyn, M. Goldstein, and N. Read, *Phys. Rev. B* **86**, 245309 (2012).
- [18] P. S. Alekseev, *Phys. Rev. Lett.* **117**, 166601 (2016).
- [19] T. Scaffidi, N. Nandi, B. Schmidt, A. P. Mackenzie, and J. E. Moore, *Phys. Rev. Lett.* **118**, 226601 (2017).
- [20] B. N. Narozhny and M. Schütt, *Phys. Rev. B* **100**, 035125 (2019).
- [21] A. Lucas and K. C. Fong, *J. Phys: Condens. Matter* **30**, 053001 (2018).
- [22] B. N. Narozhny, I. V. Gornyi, A. D. Mirlin, and J. Schmalian, *Annalen der Physik* **529**, 1700043 (2017).
- [23] L. S. Levitov and G. Falkovich, *Nat. Phys.* **12**, 672 (2016).
- [24] P. S. Alekseev, A. P. Dmitriev, I. V. Gornyi, V. Y. Kachorovskii, B. N. Narozhny, M. Schütt, and M. Titov, *Phys. Rev. Lett.* **114**, 156601 (2015).
- [25] P. S. Alekseev, A. P. Dmitriev, I. V. Gornyi, V. Y. Kachorovskii, B. N. Narozhny, M. Schütt, and M. Titov, *Phys. Rev. B* **95**, 165410 (2017).
- [26] P. S. Alekseev, A. P. Dmitriev, I. V. Gornyi, V. Y. Kachorovskii, B. N. Narozhny, and M. Titov, *Phys. Rev. B* **97**, 085109 (2018).
- [27] P. S. Alekseev, A. P. Dmitriev, I. V. Gornyi, V. Y. Kachorovskii, B. N. Narozhny, and M. Titov, *Phys. Rev. B* **98**, 125111 (2018).
- [28] O. M. Corbino, *Nuovo Cimento* **1**, 397 (1911).
- [29] A. Tomadin, G. Vignale, and M. Polini, *Phys. Rev. Lett.* **113**, 235901 (2014).
- [30] T. Holder, R. Queiroz, and A. Stern, *Phys. Rev. Lett.* **123**, 106801 (2019).
- [31] M. Shavit, A. V. Shytov, and G. Falkovich, *Phys. Rev. Lett.* **123**, 026801 (2019).
- [32] C. Kumar, J. Birkbeck, J. A. Sulpizio, D. J. Perello, T. Taniguchi, K. Watanabe, O. Reuven, T. Scaffidi, A. Stern, A. K. Geim, et al. (2021), arXiv:2111.06412.
- [33] A. Hui, V. Oganessian, and E.-A. Kim, *Phys. Rev. B* **103**, 235152 (2021).
- [34] S. Li, A. Levchenko, and A. V. Andreev, *Phys. Rev. B* **105**, 125302 (2022).
- [35] A. Stern, T. Scaffidi, O. Reuven, C. Kumar, J. Birkbeck, and S. Ilani (2021), arXiv:2110.15369.
- [36] O. E. Raichev (2022), arXiv:2202.06623.
- [37] B. N. Narozhny, *Annals of Physics* **411**, 167979 (2019).
- [38] B. N. Narozhny, I. V. Gornyi, M. Titov, M. Schütt, and A. D. Mirlin, *Phys. Rev. B* **91**, 035414 (2015).
- [39] G. Y. Vasileva, D. Smirnov, Y. L. Ivanov, Y. B. Vasilyev, P. S. Alekseev, A. P. Dmitriev, I. V. Gornyi, V. Y. Kachorovskii, M. Titov, B. N. Narozhny, et al., *Phys. Rev. B* **93**, 195430 (2016).
- [40] A. B. Kashuba, *Phys. Rev. B* **78**, 085415 (2008).
- [41] M. Müller and S. Sachdev, *Phys. Rev. B* **78**, 115419 (2008).
- [42] M. S. Foster and I. L. Aleiner, *Phys. Rev. B* **79**, 085415 (2009).
- [43] M. Schütt, P. M. Ostrovsky, I. V. Gornyi, and A. D. Mirlin, *Phys. Rev. B* **83**, 155441 (2011).
- [44] U. Briskot, M. Schütt, I. V. Gornyi, M. Titov, B. N. Narozhny, and A. D. Mirlin, *Phys. Rev. B* **92**, 115426 (2015).
- [45] J. M. Link, B. N. Narozhny, E. I. Kiselev, and J. Schmalian, *Phys. Rev. Lett.* **120**, 196801 (2018).
- [46] B. N. Narozhny, I. V. Gornyi, and M. Titov, *Phys. Rev. B* **104**, 075443 (2021).
- [47] M. P. Marder, *Condensed Matter Physics* (Wiley, 2010).
- [48] B. N. Narozhny and I. V. Gornyi, *Frontiers in Physics* **9**, 108 (2021).
- [49] M. Müller, J. Schmalian, and L. Fritz, *Phys. Rev. Lett.* **103**, 025301 (2009).
- [50] B. N. Narozhny, I. V. Gornyi, and M. Titov, *Phys. Rev. B* **103**, 115402 (2021).
- [51] Gall, V. and Narozhny, B. N. and Gornyi, I. V., unpublished.
- [52] M. Kamada, V. Gall, J. Sarkar, M. Kumar, A. Laitinen, I. Gornyi, and P. Hakonen, *Phys. Rev. B* **104**, 115432 (2021).
- [53] M. Kumar, A. Laitinen, and P. Hakonen, *Nature Communications* **9**, 2776 (2018).
- [54] B. L. Altshuler and A. G. Aronov, in *Electron-Electron Interactions in Disordered Systems*, edited by A. L. Efros and M. Pollak (North-Holland, Amsterdam, 1985).
- [55] G. Zala, B. N. Narozhny, and I. L. Aleiner, *Phys. Rev. B* **64**, 214204 (2001).
- [56] L. D. Landau and E. M. Lifshitz, *Fluid Mechanics* (Pergamon Press, London, 1987).
- [57] B. N. Narozhny, I. L. Aleiner, and A. Stern, *Phys. Rev. Lett.* **86**, 3610 (2001).
- [58] I. S. Burmistrov, M. Goldstein, M. Kot, V. D. Kurilovich, and P. D. Kurilovich, *Phys. Rev. Lett.* **123**, 026804 (2019).
- [59] D. Halbertal, J. Cuppens, M. Ben Shalom, L. Embon, N. Shadmi, Y. Anahory, H. R. Naren, J. Sarkar, A. Uri, Y. Ronen, et al., *Nature* **539**, 407 (2016).
- [60] D. Halbertal, M. Ben Shalom, A. Uri, K. Bagani, A. Y. Meltzer, I. Markus, Y. Myasoedov, J. Birkbeck, L. S. Levitov, A. K. Geim, et al., *Science* **358**, 1303 (2017).
- [61] A. Aharon-Steinberg, A. Marguerite, D. J. Perello, K. Bagani, T. Holder, Y. Myasoedov, L. S. Levitov, A. K. Geim, and E. Zeldov, *Nature* **593**, 528 (2021).
- [62] L. Ella, A. Rozen, J. Birkbeck, M. Ben-Shalom, D. Perello, J. Zultak, T. Taniguchi, K. Watanabe, A. K. Geim, S. Ilani, et al., *Nat. Nanotechnol.* **14**, 480 (2019).

- [63] B. N. Narozhny, I. V. Gornyi, and M. Titov, Phys. Rev. B **104**, 075443 (2021), URL <https://link.aps.org/doi/10.1103/PhysRevB.104.075443>.
- [64] F. M. D. Pellegrino, I. Torre, and M. Polini, Phys. Rev. B **96**, 195401 (2017), URL <https://link.aps.org/doi/10.1103/PhysRevB.96.195401>.
- [65] M. Kamada, V. Gall, J. Sarkar, M. Kumar, A. Laitinen, I. Gornyi, and P. Hakonen, Phys. Rev. B **104**, 115432 (2021), URL <https://link.aps.org/doi/10.1103/PhysRevB.104.115432>.
- [66] M. Shavit, A. Shytov, and G. Falkovich, Phys. Rev. Lett. **123**, 026801 (2019), URL <https://link.aps.org/doi/10.1103/PhysRevLett.123.026801>.
- [67] S. Li, A. Levchenko, and A. V. Andreev, Phys. Rev. B **105**, 125302 (2022), URL <https://link.aps.org/doi/10.1103/PhysRevB.105.125302>.